A hierarchy of signals regulates entry of membrane proteins into the ciliary membrane domain in epithelial cells

Stephen S. Francis,[1,2] Jeff Sfakianos,[2] Bryan Lo,[2] and Ira Mellman[2]

[1]Department of Cell Biology, Yale University School of Medicine, New Haven, CT 06510
[2]Genentech, Inc., San Francisco, CA 94080

The membrane of the primary cilium is continuous with the plasma membrane but compositionally distinct. Although some membrane proteins concentrate in the cilium, others such as podocalyxin/gp135 are excluded. We found that exclusion reflects a saturable selective retention mechanism. Podocalyxin is immobilized by its PDZ interaction motif binding to NHERF1 and thereby to the apical actin network via ERM family members. The retention signal was dominant, autonomous, and transferable to membrane proteins not normally excluded from the cilium. The NHERF1-binding domains of cystic fibrosis transmembrane conductance regulator and Csk-binding protein were also found to act as transferable retention signals. Addition of a retention signal could inhibit the ciliary localization of proteins (e.g., Smoothened) containing signals that normally facilitate concentration in the ciliary membrane. Proteins without a retention signal (e.g., green fluorescent protein–glycosylphosphatidylinositol) were found in the cilium, suggesting entry was not impeded by a diffusion barrier or lipid microdomain. Thus, a hierarchy of interactions controls the composition of the ciliary membrane, including selective retention, selective inclusion, and passive diffusion.

Introduction

Ciliopathies reveal the importance of the primary cilium to human physiology (Fliegauf et al., 2007). Cilia are found on most cells of the body, including polarized epithelial cells where the membrane of the primary cilium is an extension of the apical plasma membrane. The ciliary membrane has a unique protein composition, enriched relative to the adjacent membrane in proteins involved in cilium-dependent signal transduction (Goetz and Anderson, 2010; Patel and Honoré, 2010). Some signaling proteins such as polycystin-2 and somatostatin receptor 3 are thought to possess cilium-specific targeting signals that specify selective transport (Geng et al., 2006; Berbari et al., 2008), and the ciliary membrane is thought to comprise a distinct lipid environment that may also control membrane protein content (Vieira et al., 2006; Janich and Corbeil, 2007). It is not known how or when the specialization of the ciliary membrane occurs, nor is it clear the extent to which the ciliary membrane contains or excludes other plasma membrane proteins.

The plasma membrane of polarized epithelial cells is divided into apical and basolateral domains separated by the tight junction diffusion barrier (Mellman and Nelson, 2008). Pioneering freeze-fracture EM studies identified a structure at the base of the cilium, the "ciliary necklace" (Gilula and Satir, 1972), which was imagined to play a similar role in isolating the membrane of the primary cilium from the adjacent plasma membrane. Lacking intercellular junctions, the necklace appears more analogous to the barrier at the axon initial segment of neurons, which separates the axonal from the somatodendritic plasma membranes (Winckler et al., 1999). Recently, Septin 2 has been proposed as a component of the ciliary barrier (Hu et al., 2010), although it is unclear whether the barrier performs the same fence function as the tight junction or axon initial segment. Consistent with a fence is evidence of a direct vesicular

Correspondence to Ira Mellman: mellman.ira@gene.com

Abbreviations used in this paper: CBP, Csk-binding protein; CFTR, cystic fibrosis transmembrane conductance regulator; CMD, ciliary membrane domain; GPI, glycosylphosphatidylinositol; IP, immunoprecipitation; NHERF, Na^+/H^+ exchanger 3 regulatory factor; SEM, scanning EM; shRNA, short hairpin RNA; Smo, Smoothened.

The Rockefeller University Press $30.00
J. Cell Biol. Vol. 193 No. 1 219–233
www.jcb.org/cgi/doi/10.1083/jcb.201009001

transport pathway that is required to deliver axonemal components to build the primary cilium and that could circumvent a barrier if membrane proteins were delivered by this route (Rogers et al., 2004; Nachury et al., 2007; Yoshimura et al., 2007; Zuo et al., 2009). However, a recent study has demonstrated that Smoothened (Smo), a signaling protein active in the cilium, reaches the ciliary membrane by lateral movement, arguing against an entry barrier at least for this protein (Milenkovic et al., 2009).

Smo is a seven-pass transmembrane protein that functions in the Hedgehog signaling pathway and localizes to the primary cilium in the presence of Hedgehog (Zhu et al., 2003; Corbit et al., 2005; Wang et al., 2009) or when overexpressed (Rohatgi et al., 2009). Before localizing to the cilium, Smo is found on the adjacent plasma membrane and then moves laterally into the ciliary membrane without endocytosis and vectorial recycling (Milenkovic et al., 2009). Ciliary enrichment could occur by passive diffusion and retention within the cilium or by active transport facilitated by an adapter, a role recently proposed for the BBSome (Jin et al., 2010). Smo's relocalization to the cilium is dependent on its association with β-arrestin, which binds to ciliary microtubule motor protein KIF3A (Kovacs et al., 2008). These interactions may assist Smo's ciliary enrichment by facilitating association with the axoneme.

In contrast, podocalyxin is an apical transmembrane protein that is excluded from the primary cilium and membrane around the base of the cilium. We refer to this podocalyxin-excluding subdomain of the apical membrane as the ciliary membrane domain (CMD). Podocalyxin was first described as the major sialomucin of glomerular podocytes (Kerjaschki et al., 1984) and has been shown to play a role in apical membrane determination in epithelial cells (Meder et al., 2005). Podocalxyin's cytoplasmic tail ends in a canonical four–amino acid PDZ-binding motif that interacts with Na^+/H^+ exchanger 3 regulatory factor (NHERF) proteins, NHERF1/ERM–binding phosphoprotein of 50 kD, and NHERF2 (Takeda et al., 2001; Li et al., 2002; Meder et al., 2005; Yu et al., 2007), which interact with the ERM family of actin-binding proteins (Reczek et al., 1997; Reczek and Bretscher, 1998; Yun et al., 1998; Terawaki et al., 2003). A complex of podocalyxin, NHERF2, and ezrin has been immunoprecipitated from glomerular extracts, strongly suggesting that podocalyxin can be linked to the actin cytoskeleton in kidney cells (Takeda et al., 2001). Further work in formaldehyde-fixed cells identified the PDZ-binding motif at the carboxy terminus of podocalyxin as necessary for exclusion from the CMD (Meder et al., 2005).

We investigated podocalyxin's CMD exclusion to determine how and when apical membrane proteins can be excluded from the primary cilium. Live cell imaging was used because we found that fixation can create CMD artifacts, which may explain contradictory results in the literature. We find that the NHERF1-ERM-actin network beneath the apical plasma membrane comprises a dominant-acting selective retention matrix that effectively excludes interacting membrane proteins from entering the CMD, contributing to the specificity of the ciliary membrane.

Results

Podocalyxin exclusion from the CMD occurs after the centrioles align under the apical membrane but before there is a primary cilium

Elongated primary cilia appear on MDCK cells ∼1 wk after cells are seeded at high density on permeable filter supports (Sfakianos et al., 2007). Imaging MDCK cells expressing GFP-tagged canine podocalyxin (GFP-PODXL) fixed 8 d after seeding revealed that GFP-PODXL was excluded from the primary cilium and an area around its base, a region we define as the CMD (Fig. 1 A), as found for endogenous podocalyxin (Meder et al., 2005). F-actin was also excluded from this region (Fig. 1 A).

Even in cells that did not appear to have a primary cilium, GFP-PODXL and F-actin were excluded from the CMD. 4 d after seeding, few primary cilia were visible by antiacetylated tubulin staining; however, GFP-PODXL showed a pattern of exclusion from the CMD similar to that seen 8 d after seeding, a pattern matched by RFP-NHERF1 (Fig. 1 B). Thus, early stages of ciliogenesis begin several days before growth of primary cilia in MDCK cells. By analyzing the distribution of GFP-PODXL on the apical surface of live cells, we determined that the CMD is established in a majority of cells within 3 d of seeding (Fig. 1 C).

We next examined the appearance of the CMD relative to the migration of the centrosome to the apical pole. The centrosome migrates to the plasma membrane as the mother centriole matures into the basal body and extends the primary cilium (Sorokin, 1962). We found that the centrioles were positioned below the center of the apical membrane within 24 h of seeding (Fig. 1 D), well before appearance of the CMD (Fig. 1 C). Thus, appearance of the GFP-PODXL exclusion zone defined formation of the CMD as a stage of ciliogenesis between migration of the centrosome and eruption of the primary cilium.

Podocalyxin has been implicated in microvillus formation (Nielsen et al., 2007), and NHERF1 knockdown results in loss of microvilli (Hanono et al., 2006). Because the CMD appeared depleted of GFP-PODXL, RFP-NHERF1, and F-actin, we expected to see gaps in the brush border corresponding to the CMD. We used scanning EM (SEM) to visualize microvilli on the apical surface and surprisingly were not able to find any gaps in the brush border (Fig. 1 E, day 4). However, once a cilium was present, it was common to see a small region at its base that was free of microvilli (Fig. 1 E, day 8). Conceivably, the dense subapical actin network must be disassembled during ciliogenesis to allow the centrosome to dock at the apical membrane. This is consistent with recent data suggesting that ciliogenesis is facilitated by actin-severing protein gelsolin or actin polymerization inhibitor cytochalasin D (Kim et al., 2010) and basal body cortactin regulator Missing-In-Metastasis (Bershteyn et al., 2010). At day 4, the reduced F-actin in the CMD may represent loss of the subapical actin network in that region and not disassembly of microvillar actin. Gaps seen in RFP-NHERF1 and GFP-PODXL distributions likely do not indicate a complete absence of these molecules in the CMD.

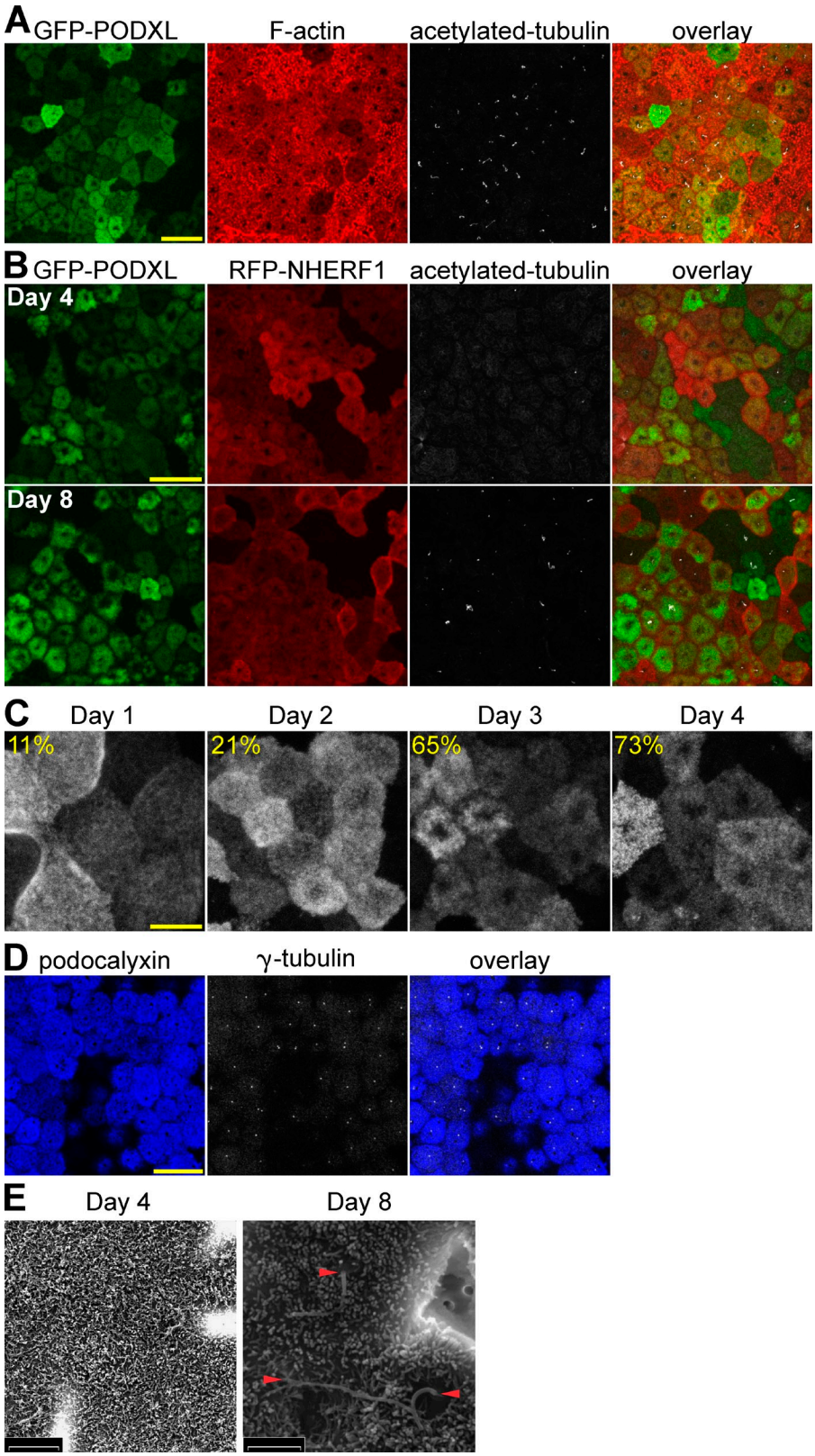

Figure 1. **Podocalyxin is excluded from the CMD before emergence of a cilium.** (A) MDCK cells expressing GFP-PODXL were grown on filters for 8 d and were fixed and stained with antiacetylated tubulin to visualize primary cilia and phalloidin to visualize F-actin. Bar, 20 µm. (B) Cells expressing GFP-PODXL and RFP-NHERF1 were fixed and stained with anti-acetylated tubulin 4 or 8 d after seeding on filters. GFP-PODXL and RFP-NHERF1 patterns are similar between days 4 and 8, but few cilia are present on day 4. Bar, 20 µm. (C) Live cells expressing GFP-PODXL were imaged and individually scored for the appearance of a GFP-PODXL exclusion zone in the center of the apical membrane. Three fields of cells were counted for each of two experiments, and the percentage of cells with apparent exclusion zones appears on each image. On day 1, only 16/150 cells appeared to have a GFP-PODXL exclusion zone. The fraction rose on day 2 (46/214) and dramatically increased on day 3 (166/257) before reaching a plateau on day 4 (182/250). Images were collected with identical microscope settings. Bar, 10 µm. (D) 24 h after seeding on a filter, cells were fixed and stained with anti–γ-tubulin to visualize centrioles and anti-gp135 to visualize endogenous podocalyxin. Centrioles are aligned below the center of the apical membrane before podocalyxin is excluded from the CMD. Small podocalyxin exclusion zones are only seen in fixed samples. Images represent a single confocal plane. Bar, 20 µm. (E) SEM imaging of cells 4 d after seeding surprisingly shows microvilli in the CMD. After 8 d, an area at the base of primary cilia (arrowheads) is free of microvilli. Images in A–C are projected z stacks. Bars: (left) 5 µm; (right) 2 µm.

The PDZ-binding motif in the cytoplasmic tail of GFP-PODXL is necessary for its exclusion from the CMD and from the cilium

It has previously been shown that the PDZ-binding motif at the end of the cytoplasmic tail of podocalyxin is necessary for its restricted distribution in the apical membrane (Meder et al., 2005). This motif has also been shown to bind to members of the NHERF family (Takeda et al., 2001; Li et al., 2002; Meder et al., 2005; Yu et al., 2007). Consistent with these findings, deletion of the four–amino acid PDZ-binding motif of GFP-PODXL

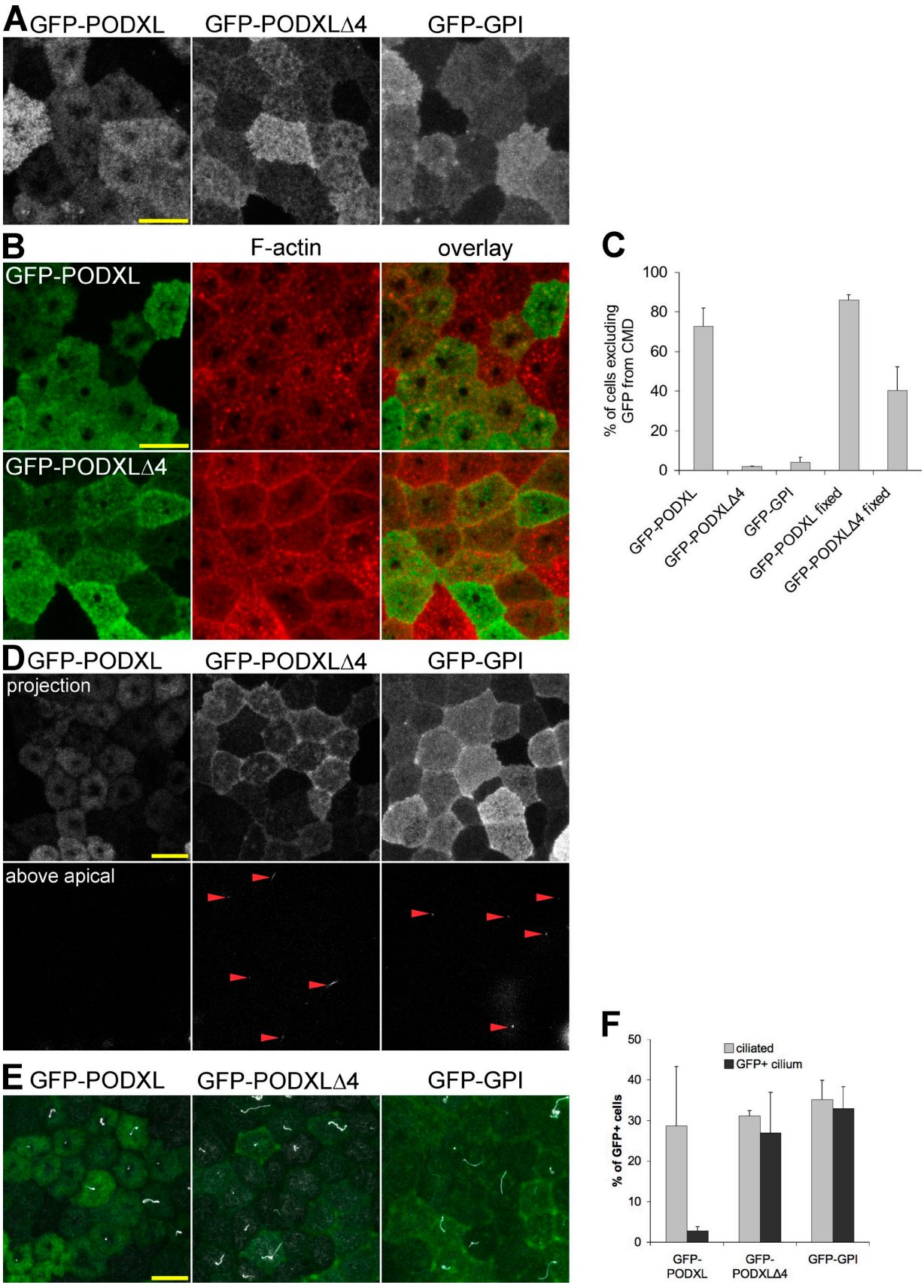

Figure 2. **GFP-PODXLΔ4 and GFP-GPI are found in the CMD and cilia of live MDCK cells, but fixation can create the appearance of CMD exclusion.** (A) Live cells expressing GFP-PODXLΔ4 or GFP-GPI were imaged 4 d after seeding and, in contrast to GFP-PODXL, failed to show exclusion from the CMD. Images were collected with microscope settings identical to Fig. 1 C. GFP-PODXL day 4 image from Fig. 1 C is shown for comparison. (B) Paraformaldehyde-fixed

(GFP-PODXLΔ4) was sufficient to allow it access to the CMD (Fig. 2 A). However, the appearance of GFP-PODXLΔ4 was altered by fixation (Fig. 2 B), and the extent of CMD exclusion observed was substantially higher in fixed cells (Fig. 2 C). GFP-glycosylphosphatidylinositol (GPI), a construct consisting of GFP tethered to the outer leaflet of the apical membrane by GPI and previously reported as excluded from the cilium in fixed cells (Vieira et al., 2006; Hu et al., 2010), also had its distribution altered by fixation (not depicted) and was readily detected in the CMD and cilium in live cells (Fig. 2, A, C, and D). In our figures, images of fixed cells are in color, and images of live cells are grayscale.

To determine whether CMD exclusion implied exclusion from the primary cilium, we looked for GFP-PODXL in extended cilia. Live cells were used to avoid fixation artifacts, so cilia were defined morphologically as projections extending at least 2 µm from the apical pole. As shown in Fig. 2 (D and F), GFP-positive cilia were observed on cells expressing GFP-PODXLΔ4 and GFP-GPI, but very few GFP-positive cilia were found on cells expressing GFP-PODXL. GFP-positive cilia are most easily appreciated in a z stack, where their extension above the apical plasma membrane can be traced. To ensure the expression of GFP-PODXL was not inhibiting ciliogenesis, we also fixed cells and stained acetylated tubulin to visualize cilia (Fig. 2 E). We found similar numbers of cilia in all cell lines (Fig. 2 F, ciliated). Because GFP-PODXL was excluded from both the CMD and primary cilium in live cells, whereas GFP-PODXLΔ4 and GFP-GPI were found in both, we conclude that exclusion from the CMD represents exclusion from the primary cilium.

Podocalyxin is selectively retained outside the CMD by NHERF1

Podocalyxin has been reported to bind to both NHERF1 and NHERF2 (Takeda et al., 2001; Li et al., 2002; Meder et al., 2005; Yu et al., 2007). GFP-NHERF2 was shown to be excluded from the CMD in MDCK cells (Meder et al., 2005), and here we show that RFP-NHERF1 has a similar distribution (Fig. 1 B). To investigate whether NHERF1 or NHERF2 had a functional role in determining podocalyxin distribution on the apical membrane, expression of NHERF1, the predominant NHERF protein in MDCK cells (Schmieder et al., 2004), was almost completely knocked down using short hairpin RNA (shRNA; Fig. 3 A). As shown in Fig. 3 (B–E), knockdown of NHERF1 resulted in GFP-PODXL entry into both the CMD and the primary cilium. Thus, full-length podocalyxin is not excluded from the CMD because of a factor inside the CMD, an exclusionary lipid microdomain, or a diffusion barrier at the base of the cilium, but rather because NHERF1 retains it outside the CMD.

We next asked whether interaction with NHERF1 controlled the lateral mobility of GFP-PODXL. By FRAP, full-length GFP-PODXL appeared relatively immobile, with only 20% of initial fluorescence reappearing in bleached regions after 120 s (Fig. 4, A and B). In contrast, GFP-PODXLΔ4 exhibited markedly enhanced mobility with a substantially higher mobile fraction than GFP-PODXL. To determine whether podocalyxin's immobilization was dependent on NHERF1, FRAP of NHERF1 knockdown cells was measured. As expected, the mobile fraction of full-length GFP-PODXL after NHERF1 knockdown was identical to that observed for GFP-PODXLΔ4 in control cells (Fig. 4, A and B). Thus, it appears that interaction with NHERF1 is responsible for immobilizing GFP-PODXL outside the CMD at the apical surface of MDCK cells.

Even when GFP-PODXL was not linked to the cytoskeleton by NHERF1, its mobility was less than that of GFP-GPI (Fig. 4, A and B), a molecule that freely diffuses in the outer leaflet of the plasma membrane. The lower mobility of GFP-PODXLΔ4 relative to GFP-GPI may be the result of podocalyxin's extracellular domain or non–PDZ-related interactions of its cytoplasmic tail.

The PDZ interaction domain of podocalyxin's cytoplasmic tail functions autonomously

To find structural elements that mediate CMD exclusion, we transferred portions of podocalyxin to CEACAM1/gp114, a protein that is evenly distributed across the apical plasma membrane of MDCK cells (Balcarova-Ständer et al., 1984; Füllekrug et al., 2006). For this study, we chose to use splice variant CEACAM1-1L (Kammerer et al., 2007) as the foundation for GFP constructs containing portions of the podocalyxin cytoplasmic domain or other proteins because it has the smallest extracellular domain and a cytoplasmic tail the same length as podocalyxin. GFP-tagged CEACAM1-1L (GFP-CEACAM1) was delivered efficiently to the apical membrane and was not excluded from the CMD (Fig. 5, A and B). By FRAP, GFP-CEACAM1 was highly mobile, with recovery similar to GFP-GPI (Fig. 5, C and D).

cells expressing GFP-PODXL (top row) or GFP-PODXLΔ4 (bottom row) were stained with phalloidin 4 d after seeding. GFP-PODXLΔ4 appeared to be excluded from the CMD in many cells. (C) Cells expressing GFP-PODXL, GFP-PODXLΔ4, or GFP-GPI were imaged and individually scored for the appearance of an exclusion zone. In live cells, GFP-PODXL was excluded from the CMD in 182/250 cells scored, in contrast to GFP-PODXLΔ4 (5/276) and GFP-GPI (11/269). In fixed cells, GFP-PODXL was still excluded from the CMD in most cells (209/243), but the fraction of cells that also excluded GFP-PODXLΔ4 increased from <5 to 40% (82/204). (D) Images of live cells 12 d after seeding on filters show that GFP-PODXLΔ4 and GFP-GPI are present in both the CMD and ciliary membrane. (top row) Z stacks of the apical membrane of live cells expressing GFP-PODXL, GFP-PODXLΔ4, or GFP-GPI were projected into a single image. Images were collected with identical microscope settings to Fig. 1 C, but at lower digital zoom. (bottom row) Single confocal sections above the apical membrane were taken from the z stacks in the top row, and image brightness was increased. Visible cilia are labeled with arrowheads. (E) Cells expressing GFP-PODXL, GFP-PODXLΔ4, or GFP-GPI (green) were fixed and stained with antiacetylated tubulin (white) to image primary cilia 12 d after seeding on filters. (F) Cilia longer than 2 µm extending from GFP-positive cells were counted in five fields in each of two experiments. In fixed cells, cilia were identified by antiacetylated tubulin (ciliated); in live cells, cilia were identified as GFP-positive projections from the center of the apical membrane (GFP + cilium). Scoring GFP-PODXL–expressing cells, 54/188 fixed cells were ciliated, but only 4/144 live cells had a GFP-positive cilium. In contrast, GFP-PODXLΔ4–expressing cells had similar numbers of cilia that could be detected using the two methods (24/77 fixed and 34/126 live), as did GFP-GPI–expressing cells (77/219 fixed and 64/194 live). Images in A, B, and E are projections of z stacks. Error bars represent standard deviation between experiments. Bars, 10 µm.

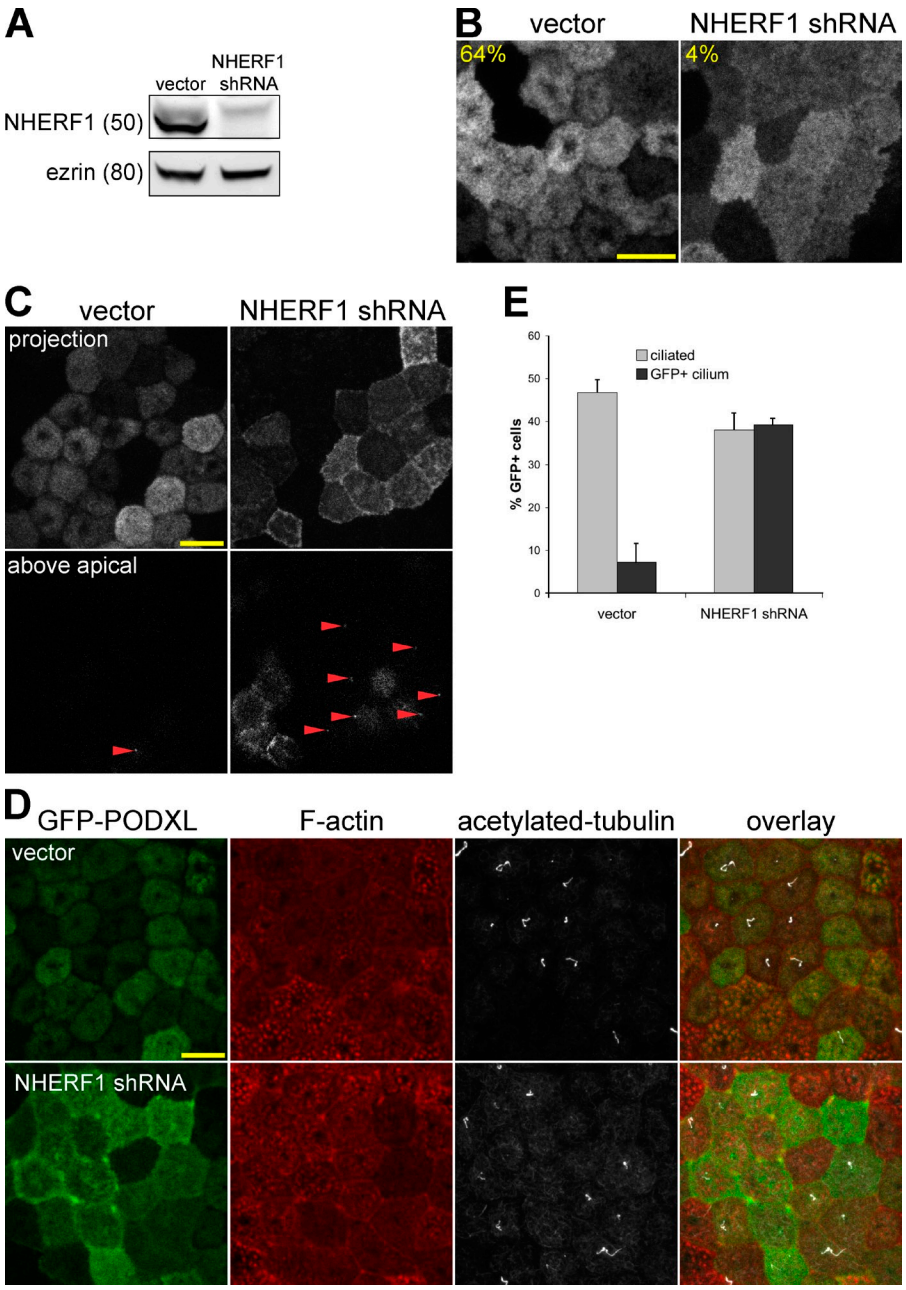

Figure 3. **CMD exclusion of GFP-PODXL is dependent on NHERF1.** (A) NHERF1 was knocked down in GFP-PODXL cells (NHERF1 shRNA) using a retroviral shRNA system. Control cells expressing GFP-PODXL (vector) were retrovirally transduced with a puromycin resistance plasmid without an shRNA sequence. Cell lysates were blotted with anti-NHERF1 and antiezrin antibodies. Molecular mass is indicated in kilodaltons. (B) Live imaging of cells 4 d after seeding revealed that control cells (vector) exclude GFP-PODXL from the CMD but NHERF1 shRNA cells do not. Exclusion was quantified as in Fig. 1 C, and the percentage of cells excluding GFP-PODXL from the CMD appears on each image. 148/230 control cells (vector) excluded GFP-PODXL from the CMD, whereas very few cells expressing NHERF1 shRNA (8/186) excluded GFP-PODXL. Images were collected with identical microscope settings to Fig. 1 C. (C) Knocking down NHERF1 allowed GFP-PODXL to enter primary cilia. Cells were imaged live 12 d after seeding on filters. (top row) Z stacks of the apical membrane of control (vector) or NHERF1 shRNA live cells expressing GFP-PODXL were projected into a single image. Images were collected with identical microscope settings to Fig. 1 C, but at lower digital zoom. (bottom row) Single confocal sections above the apical membrane were taken from the z stacks in the top row, and image brightness was increased. Visible cilia are labeled with arrowheads. (D) 12 d after seeding, NHERF1 shRNA and control cells (vector) were fixed and stained with phalloidin and antiacetylated tubulin. GFP-PODXL is found in the CMD of NHERF1 shRNA cells, but actin is still excluded from the CMD, and primary cilia appear to grow normally. (E) 100/214 control cells (vector) had a cilium detected by antiacetylated tubulin after fixation, whereas only 15/208 live cells had a GFP-PODXL–positive cilium. After NHERF1 knockdown, similar numbers of cilia could be detected using each method (74/194 fixed and 57/145 live). Images in B and D are projections of z stacks. Error bars represent standard deviation between experiments. Bars, 10 µm.

We first added only the four–amino acid PDZ-binding motif from podocalyxin to the carboxy terminus of GFP-CEACAM1 (GFP-CEACAM1-DTHL). GFP-CEACAM1-DTHL was not retained outside the CMD (Fig. 5, A and B), and its mobility measured by FRAP was similar to GFP-CEACAM1 (Fig. 5, C and D). In contrast, replacement of the last 62 amino acids of GFP-CEACAM1 with those of PODXL (GFP-CEACAM1-PODXL) was sufficient to exclude the construct from the CMD (Fig. 5, A and B) and to reduce its mobile fraction in the apical membrane (Fig. 5, C and D). Subsequent deletion of the PDZ-binding motif from the cytoplasmic tail of GFP-CEACAM1-PODXL (GFP-CEACAM1-PODXLΔ4) eliminated these effects (Fig. 5, A–D). Finally, immunoprecipitation (IP) of the podocalyxin and CEACAM1 constructs confirmed that GFP-CEACAM1-PODXL interacted with NHERF1 similarly to GFP-PODXL, whereas the constructs that were not excluded from the CMD did not (Fig. 5 E). Together, these results indicate that the NHERF1-dependent retention activity associated with the podocalyxin cytoplasmic tail can be transferred to another protein autonomously. Although the activity required more than just the last four residues comprising the canonical PDZ-binding motif, these motifs have previously been shown to be context dependent (Maday et al., 2008).

To determine whether the properties of podocalyxin's cytoplasmic tail are unique, we tested the cytoplasmic domains of other NHERF1-binding membrane proteins for their ability to alter the distribution and mobility of GFP-CEACAM1. Cystic fibrosis transmembrane conductance regulator (CFTR) and Csk-binding protein (CBP) are both membrane proteins reported to be immobilized by their interactions with NHERF1

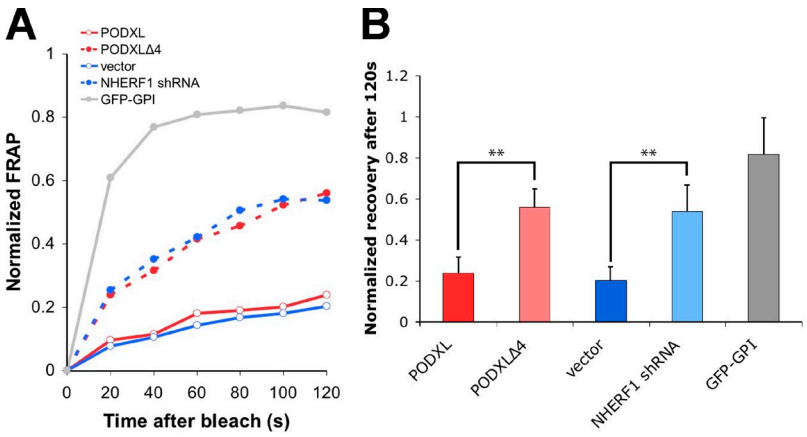

Figure 4. **GFP-PODXL mobility is increased by PDZ-binding motif deletion or NHERF1 knockdown.** (A) FRAP measurements on cells 4 d after seeding show that the lateral mobility of GFP-PODXL was increased either by deletion of the last four amino acids of its cytoplasmic tail (GFP-PODXLΔ4) or by knockdown of NHERF1 (NHERF1 shRNA). GFP-GPI is thought to freely diffuse in the membrane and recovers faster than the GFP-PODXL constructs. (B) FRAP measurements taken 120 s after photobleaching show a significant difference in FRAP between GFP-PODXL and GFP-PODXLΔ4 ($P < 0.005$). A similar difference was found between FRAP of GFP-PODXL after shRNA knockdown of NHERF1 and vector controls ($P < 0.005$). Values are means of FRAP measurements from 10 cells for GFP-GPI, GFP-PODXL, GFP-PODXLΔ4, and GFP-GPI and 8 cells for vector and NHERF1 shRNA. Error bars represent standard deviation between measurements.

(Brdicková et al., 2001; Itoh et al., 2002; Haggie et al., 2004, 2006; Chen et al., 2006). We added the final 32 amino acids of each protein to GFP-CEACAM1 to create GFP-CEACAM1-CFTR and GFP-CEACAM1-CBP. GFP-CEACAM1-CFTR was excluded from the CMD, but not after removal of the last four amino acids of its tail (GFP-CEACAM1-CFTRΔ4; Fig. 5, A and B). Similar observations were made of GFP-CEACAM1-CBP (not depicted). Both of the full-length constructs had lower FRAP than GFP-CEACAM1-PODXL, showing that they were even more effective than the podocalyxin cytoplasmic tail at restricting the mobility of GFP-CEACAM1. Yet, after removal of their PDZ-binding motifs, both GFP-CEACAM1-CFTRΔ4 and GFP-CEACAM1-CBPΔ4 exhibited the same high rate of FRAP as unmodified GFP-CEACAM1 (Fig. 5, C and D).

As a further test of the specificity of podocalyxin retention, we expressed GFP-CEACAM1-PODXL at high levels to determine whether exogenous protein would compete with endogenous podocalyxin for the limited pool of NHERF1. If so, the excess podocalyxin would be expected to enter the CMD. We generated cell lines that highly expressed either GFP-CEACAM1-PODXL or GFP-CEACAM1-PODXLΔ4 and stained the cells for endogenous podocalyxin (Fig. 5, F and G). Cells expressing high levels of GFP-CEACAM1-PODXL did not show CMD exclusion of either GFP-CEACAM1-PODXL or endogenous podocalyxin, whereas neighboring cells without GFP-CEACAM1-PODXL excluded endogenous podocalyxin from the CMD. High expression of GFP-CEACAM1-PODXLΔ4 did not affect the distribution of endogenous podocalyxin. We conclude that the selective retention mechanism is saturable and that there is not an additional barrier to endogenous podocalyxin's entry to the CMD or cilium.

A link to ERMs or actin results in CMD exclusion even with NHERF1 knockdown

In an additional set of experiments, we asked whether the direct fusion of domains from either NHERF1 or its presumptive binding partner ezrin would substitute for podocalyxin's PDZ interaction domain in programming retention outside the CMD. A similar approach was recently reported in an analysis of endocytic recycling of β2-adrenergic receptor (Lauffer et al., 2009). We transferred the ERM-binding domain of NHERF1 to GFP-CEACAM1 (GFP-CEACAM1-NHERF1) and found that it acquired the membrane distribution and mobility of GFP-PODXL (Fig. 6, A–D). Similarly, addition of the actin-binding domain of ezrin to GFP-CEACAM1 (GFP-CEACAM1-ezrin) resulted in CMD exclusion and significantly reduced mobile fraction, as judged by FRAP (Fig. 6, A–D).

Retention of GFP-CEACAM1-NHERF1 should be independent of endogenous NHERF1 because the construct can interact with ERMs directly using its NHERF1 ERM-binding domain, unless the retention matrix itself is dependent on NHERF1. To test this, we used shRNA to knock down expression of NHERF1 in our GFP-CEACAM1-NHERF1 cell line. Despite a nearly complete knockdown of endogenous NHERF1 (Fig. 6 B), CMD exclusion was not affected (Fig. 6, A and C). Endogenous NHERF1 was also not required to restrict the lateral mobility of GFP-CEACAM1-NHERF1 (Fig. 6, D and E). Thus, the retention matrix itself does not require NHERF1, which appears to act only as an adapter that restricts lateral movement of interacting membrane proteins by linking them to ERMs and actin.

Smo is retained outside the cilium by addition of a retention signal

Smo is a transmembrane protein in the Hedgehog signaling pathway that depends on ciliary localization for its signaling function (Corbit et al., 2005). The mechanism by which Smo is specifically targeted to the cilium is not understood, but a recent study has suggested that Smo enters the cilium by lateral transport (Milenkovic et al., 2009). In this process, Smo is delivered to the plasma membrane and then moves laterally to the ciliary membrane either by passive diffusion or active transport. This is an alternative to direct delivery from an intracellular pool to the ciliary membrane, which is also reported to be the mechanism of selective accumulation of Smo in the cilium (Wang et al., 2009).

If Smo is delivered to the apical membrane outside the CMD, it could be retained there by addition of NHERF1's ERM-binding domain, similar to our GFP-CEACAM1-NHERF1 construct. To test this, we generated a Smo construct with a GFP tag on the extracellular amino terminus and NHERF1's ERM-binding domain on the cytoplasmic carboxy terminus (GFP-Smo-NHERF1). To ensure that the addition of the NHERF1 domain did not simply inhibit ciliary transport of Smo, we also generated

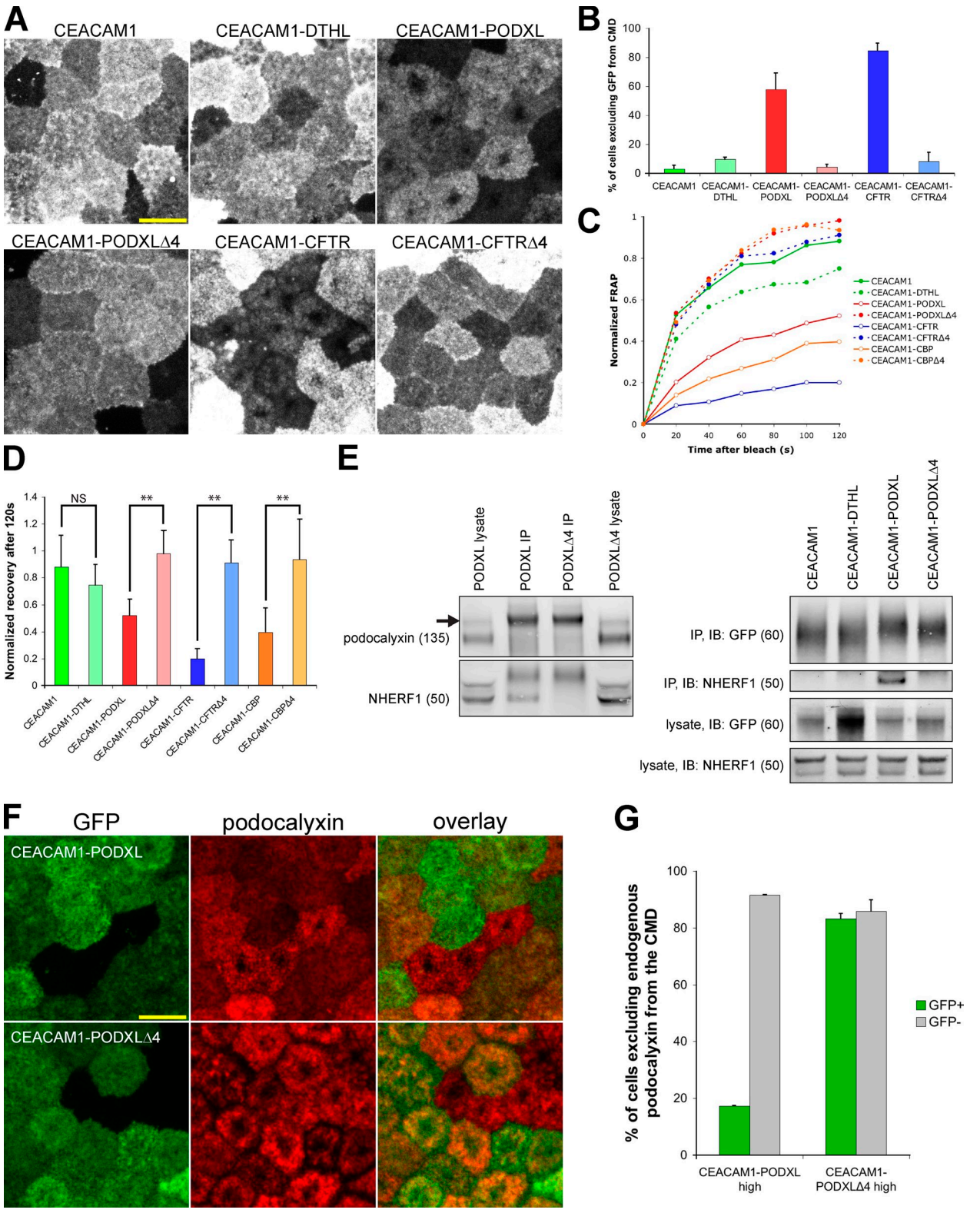

Figure 5. **CEACAM1 can be excluded from the CMD by adding tails from NHERF1-binding proteins.** (A) GFP-CEACAM1–based constructs differ in their exclusion from the CMD 4 d after seeding. Images were collected with identical microscope settings to Fig. 1 C. (B) Cells were scored for GFP exclusion from the CMD as in Fig. 1 C. Only 5/169 cells appeared to exclude GFP-CEACAM1 from the CMD, and GFP-CEACAM1-DTHL (13/135), GFP-CEACAM1-PODXLΔ4 (10/237), and GFP-CEACAM1-CFTRΔ4 (12/148) were similar, whereas GFP-CEACAM1-PODXL (146/253) and GFP-CEACAM1-CFTR (94/111) were excluded from the CMD in most cells. (C) FRAP measurements indicated that GFP-CEACAM1 constructs that were excluded from the CMD were also less mobile in the apical membrane. (D) There was no significant difference between FRAP measurements of GFP-CEACAM1 and GFP-CEACAM1-DTHL after 120 s; however, there were significant differences between GFP-CEACAM1-PODXL and GFP-CEACAM1-PODXLΔ4, GFP-CEACAM1-CFTR and GFP-CEACAM1-CFTRΔ4, and GFP-CEACAM1-CBP and GFP-CEACAM1-CBPΔ4 ($P < 0.005$). (C and D) Each FRAP value is a mean of measurements from eight cells. Error bars represent standard deviation between measurements. (E) Cells expressing GFP constructs were grown on

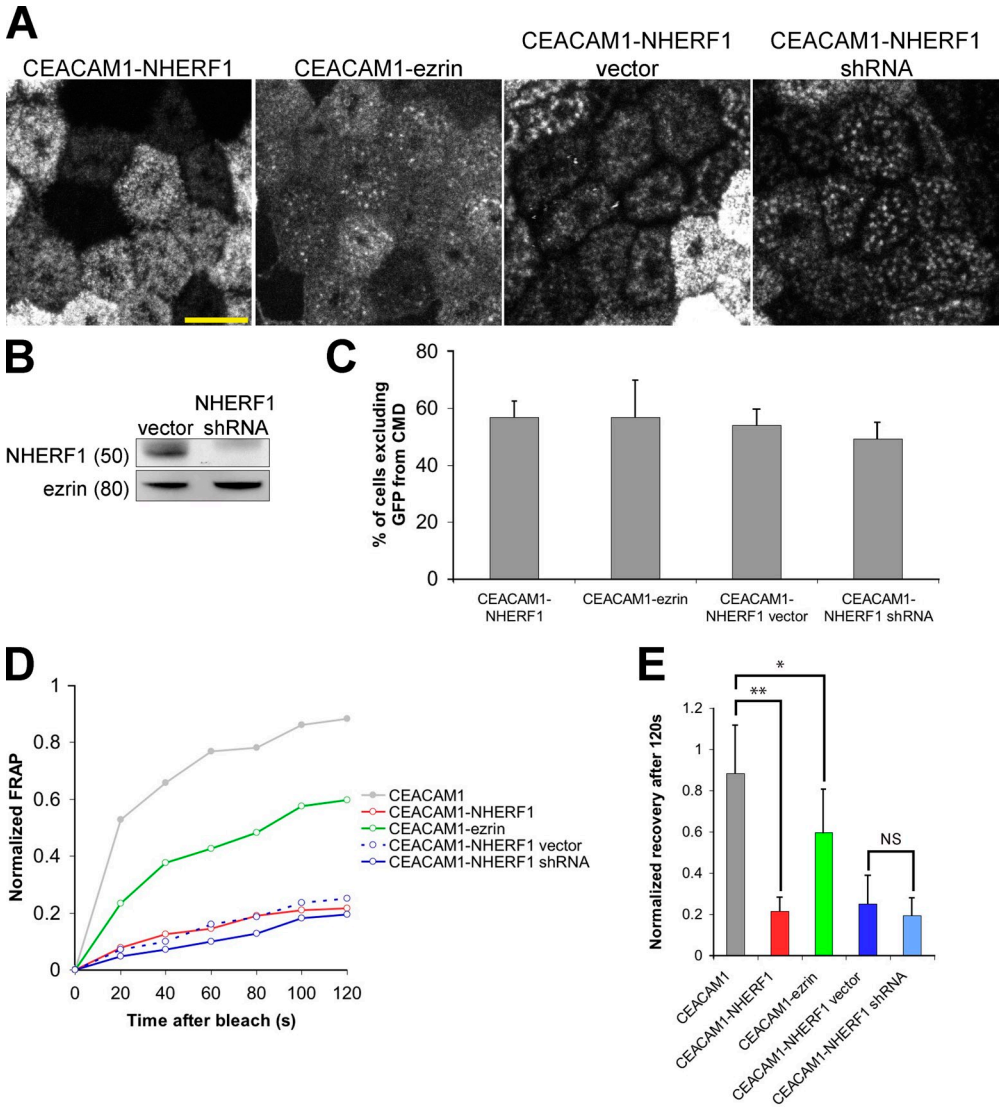

Figure 6. **CEACAM1 can be excluded from the CMD independently of NHERF1 by adding domains that bind more directly to the cytoskeleton.** (A) Addition of NHERF1's ERM-binding domain or ezrin's actin-binding domain is sufficient to exclude GFP-CEACAM1 from the CMD 4 d after seeding. NHERF1 was knocked down in GFP-CEACAM1-NHERF1 cells (GFP-CEACAM1-NHERF1 shRNA), and exclusion was similar to control cells (GFP-CEACAM1-NHERF1 vector). Images were collected with identical microscope settings to Fig. 1 C. (B) GFP-CEACAM1-NHERF1 shRNA and GFP-CEACAM1-NHERF1 vector cell lysates were blotted with anti-NHERF1 and antiezrin antibodies. Molecular mass is indicated in kilodaltons. (C) Cells were scored for GFP exclusion from the CMD as in Fig. 1 C. 113/199 cells expressing GFP-CEACAM1-NHERF1 appeared to exclude the construct from the CMD, and similar results were seen for GFP-CEACAM1-ezrin (105/185). After shRNA knockdown of NHERF1, GFP-CEACAM1-NHERF1 was excluded from the CMD in 193/393 cells, a similar ratio to cells only treated with vector (125/232). Error bars represent standard deviation between experiments. (D) FRAP measurements indicated that GFP-CEACAM1 was less mobile in the apical membrane after addition of an ERM- or actin-binding domain, and this was independent of NHERF1 knockdown. (E) There are significant differences in the FRAP measurements between GFP-CEACAM1 and both GFP-CEACAM1-NHERF1 (**, $P < 0.005$) and GFP-CEACAM1-ezrin (*, $P < 0.05$) after 120 s. No significant difference was seen in the FRAP of GFP-CEACAM1-NHERF1 after shRNA knockdown of NHERF1. GFP-CEACAM1 data are from Fig. 5 and are included as a reference. (D and E) Each FRAP value is a mean of measurements from eight cells. Error bars represent standard deviation between measurements. Images are projections of z stacks. Bars, 10 µm.

tissue culture plates and lysed when confluent. GFP constructs were immunoprecipitated from cell lysates, eluted, and Western blotted. Membranes were probed with anti-NHERF1 and either anti-GFP or anti-gp135 antibodies. The arrow to the left of the podocalyxin blot points to the GFP-PODXL band; the large band below is endogenous podocalyxin. GFP-PODXL and GFP-PODXLΔ4 lysate lanes represent 2% of the lysate used in the IP, and CEACAM1 lysate blots represent 1% of the lysate used in the IP. Molecular mass is indicated in kilodaltons. (F) Cells expressing high levels of GFP-CEACAM1-PODXL or GFP-CEACAM1-PODXLΔ4 were grown on filters for 4 d, methanol fixed, and stained for endogenous podocalyxin with anti-gp135 antibody. Podocalyxin did not appear to be excluded from the CMD in cells expressing GFP-CEACAM1-PODXL, whereas podocalyxin distribution was unaffected by expression of GFP-CEACAM1-PODXLΔ4. (G) CMD exclusion of endogenous podocalyxin was scored in cells expressing high levels of GFP-CEACAM1-PODXL or GFP-CEACAM1-PODXLΔ4 and in neighboring cells not expressing a GFP construct. Only 34/197 cells expressing GFP-CEACAM1-PODXL appeared to be excluding endogenous podocalyxin from the CMD, whereas 131/143 neighboring cells were excluding podocalyxin. The fraction of cells excluding podocalyxin was similar between those expressing GFP-CEACAM1-PODXLΔ4 (119/143) and neighbors (128/149). Images are projections of z stacks. Error bars represent standard deviation between experiments, except in D. Bars, 10 µm.

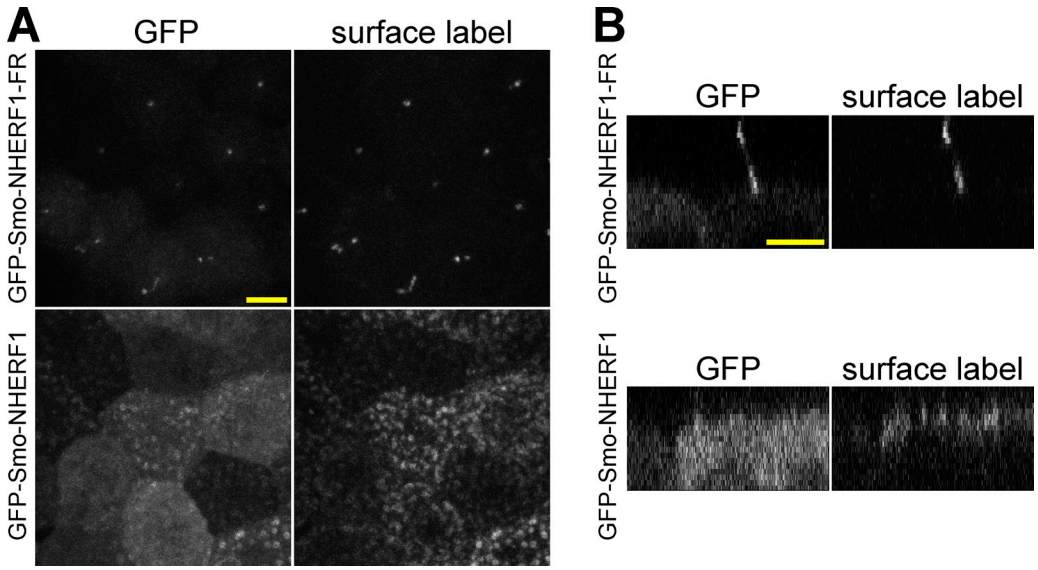

Figure 7. **Smo can be retained outside the CMD by association with the retention matrix.** Live cells expressing GFP-Smo-NHERF1-FR or GFP-Smo-NHERF1 were labeled with Alexa Fluor 647 anti-GFP on the apical side (surface label). (A) XY projections of cells expressing the ERM binding–deficient GFP-Smo-NHERF1-FR exhibit bright spots corresponding to cilia. Pairs of spots are concentrations of GFP at the base and tip of a single cilium. In contrast, Smo fused to a NHERF1 domain capable of binding ERMs (GFP-Smo-NHERF1) was localized over the entire apical plasma membrane outside the CMD. Bar, 10 µm. (B) XZ sections of cells expressing GFP-Smo-NHERF1-FR reveal cilia with an uneven distribution of GFP. Surface labeling shows GFP-Smo-NHERF1 across the apical membrane. Image brightness was increased in B. Bar, 5 µm.

a control construct (GFP-Smo-NHERF1-FR) in which a one–amino acid substitution was made in the NHERF1 domain to eliminate ERM binding (Finnerty et al., 2004). Cell lines expressing these Smo constructs were analyzed for Smo distribution by confocal microscopy. The Smo fusion constructs were not efficiently delivered to the plasma membrane, making the distribution of Smo on the cell surface difficult to determine by GFP signal alone. We therefore used anti-GFP antibody to visualize Smo on the apical surface of live cells. GFP-Smo-NHERF1-FR was localized almost entirely to the primary cilium (Fig. 7, A and B), similar to the distribution of GFP-Smo (not depicted). In contrast, GFP-Smo-NHERF1 was mostly restricted to the apical membrane with a pattern that resembled CMD exclusion with only low levels in the cilium. This result is consistent with Smo following an indirect delivery pathway to the cilium because GFP-Smo-NHERF1 was retained outside the CMD, where it was presumably first inserted in the apical membrane. It also indicates that retention outside of the CMD is cis-dominant over movement into and selective accumulation within the cilium itself.

CEACAM1 becomes enriched in the primary cilium with the addition of a microtubule-binding domain

Absent the ability to interact with the retention matrix, podocalyxin and CEACAM1 can freely enter the cilium, meaning they are not subject to a diffusion barrier at the cilium base. However, Smo is found enriched in the cilium after delivery to the apical membrane, suggesting either that it is selectively retained after passive diffusion into the cilium or that its entry is facilitated. Given the characteristic axonemal microtubule arrays found within cilia and our findings on actin-based retention, we asked whether we could cause ciliary retention of a nonciliary protein by adding a microtubule-binding element to its cytoplasmic domain. We thus generated a GFP-CEACAM1 construct fused to microtubule-associated protein tau (GFP-CEACAM1-tau). The 352–amino acid tau protein was a much larger addition to GFP-CEACAM1 than our ERM- or actin-binding domains but did not interfere with apical trafficking of the fusion protein at low expression levels. Before ciliogenesis, GFP-CEACAM1-tau was evenly distributed across the apical membrane (Fig. 8 A), and its mobility was not significantly different from GFP-CEACAM1 by FRAP (Fig. 8 B). Once a primary cilium developed, however, GFP-CEACAM1-tau appeared concentrated in the cilium relative to GFP-CEACAM1 (Fig. 8 C). These data show that a protein can be enriched in the cilium simply by association with axonemal microtubules. Thus, selective retention in the cilium, perhaps via microtubule motors such as KIF3A, may contribute to the ciliary enrichment of selected membrane proteins.

Discussion

The ciliary membrane represents a distinct, differentiated microdomain that, in epithelial cells, exists as a subregion of an already distinct apical surface. How the specificity of the ciliary membrane is generated and maintained is only now becoming clear, and our results add a fundamental new mechanism to the process. We have found that PDZ-dependent interactions of membrane proteins such as podocalyxin with NHERF1, ezrin, and actin comprise an effective retention matrix that is necessary and sufficient to impede the passive diffusion of membrane proteins from the apical surface into the CMD and membrane of the primary cilium. This retention mechanism can even prevent

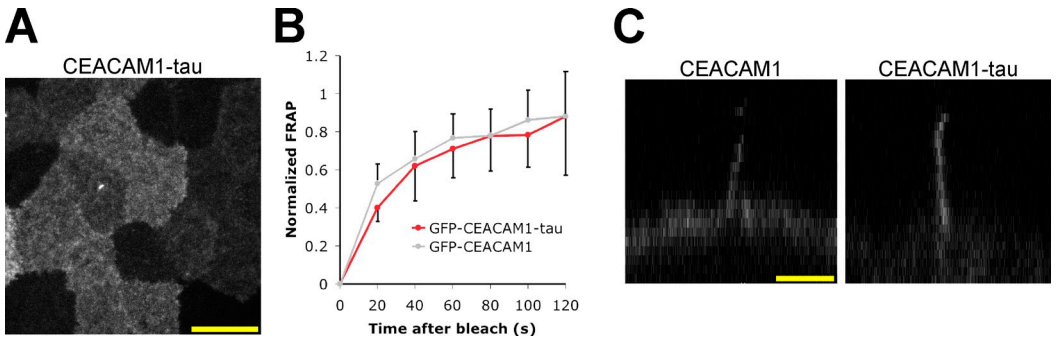

Figure 8. **GFP-CEACAM1 is concentrated in the primary cilium after addition of a microtubule-binding domain.** (A) Live cells expressing GFP-CEACAM1-tau were imaged 4 d after seeding. The image is a projection of a z stack and was collected with identical microscope settings to Fig. 1 C. Bar, 10 µm. (B) FRAP measurements of GFP-CEACAM1-tau 4 d after seeding show mobility similar to GFP-CEACAM1. GFP-CEACAM1 data are from Fig. 5 and are included as a reference. Each FRAP value is a mean of measurements from eight cells. Error bars represent standard deviation between measurements. (C) XZ sections of cells 12 d after seeding show GFP-CEACAM1-tau enriched in the cilium relative to the apical membrane, whereas GFP-CEACAM1 is evenly distributed. Bar, 3 µm.

the ciliary localization of membrane proteins such as Smo, which are normally concentrated in the cilium. Although the ciliary membrane may also be a specialized lipid environment (Vieira et al., 2006; Janich and Corbeil, 2007), this does not appear to contribute to the exclusion of apical membrane proteins. Nor does a diffusion barrier act to prevent the entry of passively diffusing proteins or of Smo, which moves laterally from its site of insertion in the plasma membrane to the cilium (Milenkovic et al., 2009). Consequently, we propose that a hierarchy of mechanisms exist that control the biogenesis of the ciliary membrane, including selective retention outside of the CMD, nonselective or selective transport from bulk plasma membrane into the CMD, and selective retention of a subset of proteins after arrival in the cilium. The latter two mechanisms likely involve specific adapters or motors such as the BBSome (somatostatin receptor 3; Jin et al., 2010), β-arrestin (Smo; Kovacs et al., 2008), and KIF3A (Crumbs3 and Smo; Fan et al., 2004; Sfakianos et al., 2007; Kovacs et al., 2008).

It seems clear why proteins involved in signaling might be selectively transported to or retained within the ciliary membrane. Why bulk plasma membrane proteins need to be excluded is less clear but may reflect the need to maintain sufficient space for signaling proteins or to prevent entry of proteins that might interfere with signaling. In this regard, it is important to note that diffusion barriers may also play an important role, although one apparently not relevant to the membrane proteins studied here. Recently, Septin 2 has been proposed to impede the movement of Smo and other ciliary membrane proteins into and out of cilia (Hu et al., 2010), a mechanism that may apply only to membrane proteins that interact with cilium-specific adapter molecules or microtubule motors (e.g., BBSome, intraflagellar transport particles, and KIF3A).

Although it was previously demonstrated that podocalyxin needs its PDZ-binding motif for cilium exclusion (Meder et al., 2005), we have defined the mechanism responsible for this effect. We found that NHERF1 is the PDZ domain protein required for podocalyxin's CMD exclusion in MDCK cells, immobilizing and retaining it in the nonciliary portions of the apical plasma membrane. NHERF2 has also been shown to bind podocalyxin (Takeda et al., 2001; Li et al., 2002) and be excluded from the CMD (Meder et al., 2005), but a functional role for NHERF2 in CMD exclusion has never been demonstrated. We predict that it could serve the same function as NHERF1 but is not endogenously expressed at high enough levels in MDCK cells to sequester a large fraction of podocalyxin outside the CMD. We also show that the addition of a NHERF1-interacting sequence from either CFTR or CBP is sufficient to cause GFP-CEACAM1 CMD exclusion, demonstrating that our findings are not exclusive to podocalyxin. We expect that all apical membrane proteins that bind to NHERF1 or are otherwise linked to the actin cytoskeleton are excluded from the CMD.

By monitoring the appearance of a GFP-PODXL–free subregion of the apical domain, we were able to identify early stages of ciliogenesis. Imaging GFP-PODXL and γ-tubulin revealed that the centrioles migrate to the future position of the primary cilium before GFP-PODXL is excluded from a central subdomain of the apical membrane. Phalloidin staining shows that F-actin is depleted from the CMD after MDCKs have been grown on filters for 4 d (Fig. 1 A); however, SEM images of 4-d-old cells do not show a corresponding lack of microvilli (Fig. 1 E), suggesting that the cleared F-actin was part of the subapical terminal web. Once a primary cilium grows days later, a small region without microvilli is present at the base of the cilium (Fig. 1 E), indicating that the basal body may continue to locally break down F-actin even after extending a cilium. The early loss of NHERF1 and podocalyxin from the CMD must represent a signal acting at the membrane to clear these proteins, but that signal does not appear to eliminate microvilli in the CMD.

Our experiments have also identified an experimental artifact that is particularly relevant to studies of the primary cilium. Fixing and permeabilizing MDCK cells can create the appearance of CMD exclusion for some apical markers, including CEACAM1 and GFP-GPI. Live cell imaging avoids this issue; however, the expression of exogenous proteins also has drawbacks when investigating retention mechanisms. Once binding sites are saturated, remaining protein is free from retention. We demonstrated this principle by expressing high levels of GFP-CEACAM1-PODXL, a construct that binds to NHERF1, which caused endogenous podocalyxin to enter the CMD (Fig. 5, F and G).

Competition for NHERF1 binding by exogenous protein expression has also been documented using CFTR (Haggie et al., 2006). To avoid saturating NHERF1-binding sites in our studies of CMD exclusion, we only used cells expressing low levels of exogenous protein (Fig. 5 E, compare GFP-PODXL band with endogenous podocalyxin band).

We have been able to enrich GFP-CEACAM1 in the primary cilium simply by adding the microtubule-associated protein tau to its cytoplasmic tail. This result demonstrates that anchoring a membrane protein to microtubules is sufficient to achieve selective localization in the cilium without the need for direct ciliary transport or a diffusion barrier at the base of the cilium. GFP-CEACAM1-tau is homogenously distributed across the apical membrane before the growth of the primary cilium and is mobile according to our FRAP measurements. Although microtubules are found throughout the cell, few are apparently close enough to the apical membrane to allow GFP-CEACAM1-tau to bind. Once the cilium grows, GFP-CEACAM1-tau can freely diffuse into the ciliary membrane, where it binds to microtubules of the axoneme. We do not expect this direct link to represent a physiological mechanism for cilium enrichment, but an indirect scaffolding system like the one that connects podocalyxin to actin can be envisioned.

Smo has been shown to be delivered to the apical membrane before concentrating in the cilium in response to Hedgehog (Milenkovic et al., 2009). Part of this mechanism is association of β-arrestin with Smo and KIF3A (Kovacs et al., 2008), which would link Smo to microtubules. This complex could transport Smo to the distal tip of the cilium, immobilize Smo by binding it to microtubules, or sequester it in the ciliary membrane by rendering it unable to cross a possible Septin 2 barrier back into the apical membrane. Other ciliary proteins might be retained in the ciliary membrane by the BBSome. The BBSome is a good candidate for a ciliary retention complex because it localizes to the cilium (Nachury et al., 2007), recognizes ciliary localization domains (Jin et al., 2010), and can indirectly link to microtubules through the dynein–dynactin complex (Kim et al., 2004).

We have found that primary cilium enrichment or exclusion of apical plasma membrane proteins can be mediated by cytoskeletal retention. Protein components that fall into this class are not dependent on a diffusion barrier for their localization. That GFP-PODXL can freely enter the CMD and cilium after dissociation from the NHERF1-ERM-actin retention matrix indicates that a ciliary fence does not restrict podocalyxin diffusion. Thus, it is now apparent that entry into, or exclusion from, the CMD involves a hierarchical interplay of several elements: (a) signals for selective inclusion within the CMD; (b) a possible barrier that impedes exit from (or less likely, entry into) the CMD; and (c) a retention matrix that prevents movement to the cilium by immobilizing nonciliary proteins in the plasma membrane.

Materials and methods

Cell culture

MDCK II and GP2-293 cells were maintained in Dulbecco's MEM with low glucose supplemented with 10% FBS, 2 mM L-glutamine, penicillin and streptomycin at 37°C, and 5% CO_2. For microscopy experiments, cells were seeded at a density of 5×10^5 for each 12-mm polycarbonate filter (Transwell; Corning). Medium was replaced daily for cells on filters.

Antibodies

The antibodies used in this study were rabbit anti–γ-tubulin (T5192; Sigma-Aldrich); mouse antiacetylated tubulin (clone 6-11B-1; Sigma-Aldrich); rabbit anti-NHERF1 (PA1-090; Thermo Fisher Scientific); rabbit anti-GFP (A11122; Invitrogen); mouse antiezrin (610602; BD); rabbit anti-GFP conjugated to Alexa Fluor 647 (Invitrogen); Alexa Fluor 488, 546, and 647 goat anti–mouse IgG and goat anti–rabbit IgG (Invitrogen); goat anti–mouse (IRDye 800CW; LI-COR Biosciences); and goat anti–rabbit (IRDye 680; LI-COR Biosciences). Anti-gp135 antibody was provided by G. Ojakian (State University of New York Downstate Medical Center, Brooklyn, NY).

Microscope

A confocal microscope with integrated photomultiplier detectors (SP5; Leica) was used to acquire images for this study. Objective lenses were a 100× 1.47 NA HCX PL APO oil immersion objective and a 63×1.40 NA HCX PL APO oil immersion objective. Application Suite software (Leica) was used to manage images.

Immunofluorescence microscopy

Cells on filters were fixed by incubation in 4% paraformaldehyde (Electron Microscopy Sciences) for 15 min at room temperature or in methanol for 20 min at –20°C. Cells were permeabilized with 0.05% saponin (Riedel-de Haën) and 2% BSA (Sigma-Aldrich) in Dulbecco's PBS with calcium and magnesium (Invitrogen). Primary and secondary antibody incubations were 1 h, and filters were washed with permeabilization buffer after each incubation. Alexa Fluor 647–conjugated phalloidin (Invitrogen) was included in the secondary incubation. Filters were mounted in SlowFade Gold (Invitrogen).

Live cell microscopy

Cells grown on filters were washed twice with cell culture medium before filters were cut from their supports and placed cell side down on a 22-mm glass bottom dish (WillCo Wells). A slice hold down (SHD-26GH/15; Warner Instruments) was placed on top of the filter, and cell culture medium was added to the dish. Cells were imaged in a 37°C chamber with 5% CO_2.

Images used to quantify CMD exclusion were acquired with a 100× objective and 2× digital zoom; images for quantitation of cilia used 3× digital zoom. To quantitate CMD exclusion, three fields of cells were scored in each of two experiments. To quantitate cilia (live and fixed), five fields of cells were scored in each of two experiments. Only cells with a mean fluorescence intensity and peak fluorescence intensity within a standard range were scored.

FRAP measurements were made using a 63× objective and 10× digital zoom. Application Suite software was used to automate the bleach of a 750-nm-diameter circle, acquisition of postbleach images, and quantitation of fluorescence recovery. The region bleached was never in the center or at the edge of the cell. To calculate recovery, the fluorescence intensity of the bleached region in the first image acquired after bleaching (time 0) was subtracted from all intensity measurements. Values were then normalized to prebleach intensity of the bleached region and scaled to the intensity of a nearby region of apical membrane to account for photobleaching during image acquisition. Traces in figures are means of FRAP calculations from at least eight cells from at least two experiments.

To visualize GFP-Smo on the cell surface, cells on filters expressing GFP-Smo constructs were washed twice with 4°C Dulbecco's PBS with calcium and magnesium (Invitrogen). PBS was completely aspirated from the apical chamber, and 200 µl of 1:100 Alexa Fluor 647–conjugated anti-GFP antibody in PBS was added to the apical chamber. Cells were incubated on ice for 5 min before being washed twice with 4°C PBS with calcium and magnesium. Filters were cut from their supports, placed on an ice-cold glass bottom dish, and weighed down with a slice anchor before an addition of 4°C PBS with calcium and magnesium to the dish. Cells were quickly imaged at room temperature. The brightness of images in Figs. 2 D, 3 C, and 7 B was increased using Photoshop CS4 (Adobe).

SEM

Samples were fixed in one-half Karnovsky's fixative (2% paraformaldehyde/2.5% glutaraldehyde in 0.1 M sodium cacodylate buffer, pH 7.4) overnight and postfixed in 1% OsO_4 for 1 h. Cells were dehydrated through a graded series of EtOH and infiltrated with hexamethyldisilazane. They were then air dried, mounted on stubs, and sputter coated with 10 nm AuPd. Samples were viewed on a microscope (XL30 ESEM; FEI).

Generation of fluorescent protein fusion constructs

GFP-GPI (Keller et al., 2001) was subcloned into pQCXIN for this study. This pQCXIN GFP-GPI plasmid became the basis for our other transmembrane GFP constructs, as cDNAs could be inserted downstream of the GFP with a stop codon upstream of the GPI linkage sequence.

Sequences for canine PODXL (GenBank/EMBL/DDBJ accession no. AY970669) and CEACAM1-1L (GenBank accession no. DQ975212) were edited to remove their signal sequences and silently add restriction enzyme sites. These edited sequences were synthesized and inserted downstream of GFP in pQCXIN GFP-GPI by Blue Heron Biotechnology.

GFP-PODXLΔ4 was made by replacing the distal tail of GFP-PODXL with synthesized oligonucleotides corresponding to the PODXL tail without its last four amino acids. GFP-CEACAM1-DTHL was made by inserting the last four codons of PODXL to the end of GFP-CEACAM1's sequence using oligonucleotides.

GFP-CEACAM1-PODXL and GFP-CEACAM1-PODXLΔ4 were created by cutting the last 62 codons from the tail of GFP-CEACAM1 and replacing them with the corresponding tail fragment of either GFP-PODXL or GFP-PODXLΔ4.

To facilitate the creation of other constructs, we created a GFP-CEACAM1 construct with the stop codon deleted (GFP-CEACAM1-NS), which allowed us to insert synthesized oligonucleotides at the end of the CEACAM1 sequence. Oligonucleotides corresponding to the carboxy-terminal 32 amino acids of CFTR (GenBank accession no. NM_000492) with or without the final four amino acids were added to GFP-CEACAM1-NS with a Glu-Phe linker to create GFP-CEACAM1-CFTR and GFP-CEACAM1-CFTRΔ4, respectively. The same process was used to create GFP-CEACAM1-CBP and GFP-CEACAM1-CBPΔ4 from the sequence of CBP (GenBank accession no. NM_018440). GFP-CEACAM1-NHERF1 and GFP-CEACAM1-ezrin were created by adding a Glu-Phe-Gly-Ala-Gly-Ala linker followed by the ERM- and actin-binding domain sequences from Lauffer et al. (2009) to the tail of GFP-CEACAM1-NS using synthesized oligonucleotides. GFP-CEACAM1-tau was created by amplifying human microtubule-associated protein tau isoform 4 (GenBank accession no. NM_016841) by PCR and ligating this fragment to the tail of GFP-CEACAM1-NS with a Glu-Phe linker.

Human Smo cDNA (GenBank accession no. BC009989) was amplified by PCR and inserted into pQCXIN GFP-GPI downstream of GFP without Smo's signal sequence or stop codon. NHERF1's ERM-binding domain was added to this Smo construct to create GFP-Smo-NHERF1. The ERM-binding domain oligonucleotide sequence was modified to substitute Arg for Phe at the location that corresponds to NHERF1 residue 355 and was added to Smo to create GFP-Smo-NHERF1-FR. Human NHERF1 cDNA (GenBank accession no. AF015926) was amplified by PCR and inserted downstream of Evrogen TagRFP in pQCXIN to create RFP-NHERF1.

Generation of cell lines stably expressing fluorescent protein constructs

To produce retroviral vectors, 10^7 GP2-293 cells were seeded on a 10-cm plate 1 d before transfection with 1.5 µg pLP-VSVG (Takara Bio Inc.) and 3 µg pQCXIN vector using Lipofectamine 2000 (Invitrogen). Cells were incubated at 32°C in complete cell culture medium during vector production. Supernatant was harvested and replaced every 24 h three times beginning 48 h after transfection. Vector-containing supernatants were pooled and debris were removed by centrifugation at 1,700 *g* for 5 min. Supernatants were used directly or aliquoted and stored at –80°C.

MDCK cells were seeded at a density of 25,000 cells per well of a 12-well dish the day before transduction with retrovirus. Cells were infected by replacing cell culture medium with up to 2 ml of viral supernatant with 10 µg/ml polybrene (American Bioanalytical), spinning at 675 *g* for 1 h, and then incubating overnight at 32°C. Cells were subsequently incubated at 37°C.

MDCK cells expressing low levels of GFP were selected using a cell sorter (FacsAria; BD). To create a low expression standard, cells transduced with GFP-PODXL retrovirus were sorted to select the least bright 10% of GFP-positive cells. Cells expressing other constructs were sorted to a similar level of fluorescence. Cell lines expressing high levels of GFP-CEACAM1-PODXL and GFP-CEACAM1-PODXLΔ4 were created by selection with 2 mg/ml G418 Sulfate (Takara Bio Inc.) and subsequently sorted to select the brightest cells. Parental MDCK cells were mixed with high-expressing cells when seeding on filters to be GFP-negative neighbors.

NHERF1 knockdown with shRNA

LTRH1-puro (Barton and Medzhitov, 2002; Sfakianos et al., 2007) was modified to allow for the insertion of an shRNA sequence into the vector by mutating the HindIII sites at positions 2872 and 4282 using site-directed mutagenesis. Oligonucleotides targeting NHERF1 mRNA (Yu et al., 2007) were synthesized, annealed, and then ligated to the LTRH1 vector between the BglII and HindIII sites.

Retroviral vectors were produced and cells were infected as described for GFP constructs. 1 d after infection, cells were selected with 8 µg/ml puromycin. To determine the degree of protein knockdown in shRNA-expressing cells, a 10-cm plate of confluent cells was washed twice with 4°C PBS with calcium and magnesium, completely aspirated, and placed on ice before treatment with 500 µl of M-PER Mammalian Protein Extraction Reagent (Thermo Fisher Scientific). After 2 min, supernatant from the plate was applied to a column (QIAshredder; QIAGEN) and centrifuged at 13,000 *g* for 1 min. The flow-through was analyzed by Western blotting after addition of NuPAGE LDS Sample Buffer (Invitrogen) and 2% 2-mercaptoethanol and incubation at 95°C for 1 min.

IP of GFP constructs

IP protocol is based on Cheeseman and Desai (2005). For each IP, 160 µl of resuspended Affi-Prep Protein A Support (Bio-Rad Laboratories) bead slurry (~110-µl bead volume) was used to make anti-GFP beads. Volumes were scaled up to prepare beads for many reactions at once. Beads were washed twice with PBST (PBS and 0.1% Tween 20), resuspended in 500 µl PBST with 80 µg anti-GFP antibody, and rotated for 1 h at room temperature. Beads were then washed twice with PBST and twice with sodium borate buffer, pH 9.0 (0.2 M sodium borate and 0.2 M boric acid), resuspended in 500 µl sodium borate buffer with 33 mM dimethyl pimelimidate, and rotated for 30 min at room temperature. To neutralize residual dimethyl pimelimidate, beads were washed once in neutralization buffer (0.2 M ethanolamine and 0.2 M NaCl, pH 8.5), rotated for 1 h in neutralization buffer, resuspended in 500 µl of neutralization buffer, and stored at 4°C.

Two 245-mm square tissue culture plates with confluent monolayers of cells were washed in 4°C PBS with calcium and magnesium and then placed on ice. Plates were scraped into 10 ml lysis buffer (100 mM NaCl, 300 mM sucrose, 3 mM $MgCl_2$, 10 mM Pipes, pH 6.8, 0.5% Triton X-100, and complete EDTA-free protease inhibitors [Roche]) centrifuged at 12,000 *g* for 30 min. Supernatant was collected, and the protein concentration was measured by bicinchoninic acid assay. 20 mg of cell lysate was added to a 100-µl bead volume of anti-GFP beads that had been washed twice with PBS/0.1% Tween and twice with lysis buffer. Lysate and beads were incubated overnight at 4°C with rotation. After overnight incubation, beads were washed five times with lysis buffer, and proteins were eluted by incubation in 100 µl of 4% SDS and 40 mM Tris, pH 8.0, at 70°C for 15 min. Eluate was mixed with NuPAGE LDS Sample Buffer (Invitrogen), and 2-mercaptoethanol was added to 2% final concentration before incubation at 95°C for 1 min and Western blot analysis.

Western blot

Protein samples in NuPAGE LDS Sample Buffer were separated by electrophoresis using NuPAGE 4–12% Bis-Tris gels (Invitrogen). Proteins were transferred to polyvinylidene fluoride membrane using the iBlot transfer system (Invitrogen). Membranes were blocked for 1 h with PBS/0.05% Tween 20/1% BSA. Primary antibodies in PBS/0.05% Tween 20/0.5% BSA were applied to membranes overnight at 4°C. Membranes were washed with PBS/0.05% Tween 20/0.5% BSA before a 1-h incubation with secondary antibodies (LI-COR Biosciences). After a final wash with PBS/0.05% Tween 20/0.5% BSA, antibody signals were visualized using a scanner (Odyssey; LI-COR Biosciences) and analyzed with Odyssey software version 3.0. Image levels were adjusted using Photoshop CS4.

The authors thank L. Rangell and M. Sun for their work on the SEM and B. Chih, C. Chalouni, the Mellman laboratory, and the Genentech research community for their advice and assistance.

Submitted: 1 September 2010
Accepted: 15 February 2011

References

Balcarova-Ständer, J., S.E. Pfeiffer, S.D. Fuller, and K. Simons. 1984. Development of cell surface polarity in the epithelial Madin-Darby canine kidney (MDCK) cell line. *EMBO J.* 3:2687–2694.

Barton, G.M., and R. Medzhitov. 2002. Retroviral delivery of small interfering RNA into primary cells. *Proc. Natl. Acad. Sci. USA*. 99:14943–14945. doi:10.1073/pnas.242594499

Berbari, N.F., A.D. Johnson, J.S. Lewis, C.C. Askwith, and K. Mykytyn. 2008. Identification of ciliary localization sequences within the third intracellular loop of G protein-coupled receptors. *Mol. Biol. Cell*. 19:1540–1547. doi:10.1091/mbc.E07-09-0942

Bershteyn, M., S.X. Atwood, W.M. Woo, M. Li, and A.E. Oro. 2010. MIM and cortactin antagonism regulates ciliogenesis and hedgehog signaling. *Dev. Cell*. 19:270–283. doi:10.1016/j.devcel.2010.07.009

Brdicková, N., T. Brdicka, L. Andera, J. Spicka, P. Angelisová, S.L. Milgram, and V. Horejsí. 2001. Interaction between two adapter proteins, PAG and EBP50: a possible link between membrane rafts and actin cytoskeleton. *FEBS Lett.* 507:133–136. doi:10.1016/S0014-5793(01)02955-6

Cheeseman, I.M., and A. Desai. 2005. A combined approach for the localization and tandem affinity purification of protein complexes from metazoans. *Sci. STKE*. 2005:pl1. doi:10.1126/stke.2662005pl1

Chen, Y., W.R. Thelin, B. Yang, S.L. Milgram, and K. Jacobson. 2006. Transient anchorage of cross-linked glycosyl-phosphatidylinositol-anchored proteins depends on cholesterol, Src family kinases, caveolin, and phosphoinositides. *J. Cell Biol.* 175:169–178. doi:10.1083/jcb.200512116

Corbit, K.C., P. Aanstad, V. Singla, A.R. Norman, D.Y.R. Stainier, and J.F. Reiter. 2005. Vertebrate Smoothened functions at the primary cilium. *Nature*. 437:1018–1021. doi:10.1038/nature04117

Fan, S., T.W. Hurd, C.J. Liu, S.W. Straight, T. Weimbs, E.A. Hurd, S.E. Domino, and B. Margolis. 2004. Polarity proteins control ciliogenesis via kinesin motor interactions. *Curr. Biol.* 14:1451–1461. doi:10.1016/j.cub.2004.08.025

Finnerty, C.M., D. Chambers, J. Ingraffea, H.R. Faber, P.A. Karplus, and A. Bretscher. 2004. The EBP50-moesin interaction involves a binding site regulated by direct masking on the FERM domain. *J. Cell Sci.* 117:1547–1552. doi:10.1242/jcs.01038

Fliegauf, M., T. Benzing, and H. Omran. 2007. When cilia go bad: cilia defects and ciliopathies. *Nat. Rev. Mol. Cell Biol.* 8:880–893. doi:10.1038/nrm2278

Füllekrug, J., A. Shevchenko, A. Shevchenko, and K. Simons. 2006. Identification of glycosylated marker proteins of epithelial polarity in MDCK cells by homology driven proteomics. *BMC Biochem.* 7:8. doi:10.1186/1471-2091-7-8

Geng, L., D. Okuhara, Z. Yu, X. Tian, Y. Cai, S. Shibazaki, and S. Somlo. 2006. Polycystin-2 traffics to cilia independently of polycystin-1 by using an N-terminal RVxP motif. *J. Cell Sci.* 119:1383–1395. doi:10.1242/jcs.02818

Gilula, N.B., and P. Satir. 1972. The ciliary necklace. A ciliary membrane specialization. *J. Cell Biol.* 53:494–509. doi:10.1083/jcb.53.2.494

Goetz, S.C., and K.V. Anderson. 2010. The primary cilium: a signalling centre during vertebrate development. *Nat. Rev. Genet.* 11:331–344. doi:10.1038/nrg2774

Haggie, P.M., B.A. Stanton, and A.S. Verkman. 2004. Increased diffusional mobility of CFTR at the plasma membrane after deletion of its C-terminal PDZ binding motif. *J. Biol. Chem.* 279:5494–5500. doi:10.1074/jbc.M312445200

Haggie, P.M., J.K. Kim, G.L. Lukacs, and A.S. Verkman. 2006. Tracking of quantum dot-labeled CFTR shows near immobilization by C-terminal PDZ interactions. *Mol. Biol. Cell*. 17:4937–4945. doi:10.1091/mbc.E06-08-0670

Hanono, A., D. Garbett, D. Reczek, D.N. Chambers, and A. Bretscher. 2006. EPI64 regulates microvillar subdomains and structure. *J. Cell Biol.* 175:803–813. doi:10.1083/jcb.200604046

Hu, Q., L. Milenkovic, H. Jin, M.P. Scott, M.V. Nachury, E.T. Spiliotis, and W.J. Nelson. 2010. A septin diffusion barrier at the base of the primary cilium maintains ciliary membrane protein distribution. *Science*. 329:436–439. doi:10.1126/science.1191054

Itoh, K., M. Sakakibara, S. Yamasaki, A. Takeuchi, H. Arase, M. Miyazaki, N. Nakajima, M. Okada, and T. Saito. 2002. Cutting edge: negative regulation of immune synapse formation by anchoring lipid raft to cytoskeleton through Cbp-EBP50-ERM assembly. *J. Immunol.* 168:541–544.

Janich, P., and D. Corbeil. 2007. GM1 and GM3 gangliosides highlight distinct lipid microdomains within the apical domain of epithelial cells. *FEBS Lett.* 581:1783–1787. doi:10.1016/j.febslet.2007.03.065

Jin, H., S.R. White, T. Shida, S. Schulz, M. Aguiar, S.P. Gygi, J.F. Bazan, and M.V. Nachury. 2010. The conserved Bardet-Biedl syndrome proteins assemble a coat that traffics membrane proteins to cilia. *Cell*. 141:1208–1219. doi:10.1016/j.cell.2010.05.015

Kammerer, R., T. Popp, S. Härtle, B.B. Singer, and W. Zimmermann. 2007. Species-specific evolution of immune receptor tyrosine based activation motif-containing CEACAM1-related immune receptors in the dog. *BMC Evol. Biol.* 7:196. doi:10.1186/1471-2148-7-196

Keller, P., D. Toomre, E. Díaz, J. White, and K. Simons. 2001. Multicolour imaging of post-Golgi sorting and trafficking in live cells. *Nat. Cell Biol.* 3:140–149. doi:10.1038/35055042

Kerjaschki, D., D.J. Sharkey, and M.G. Farquhar. 1984. Identification and characterization of podocalyxin—the major sialoprotein of the renal glomerular epithelial cell. *J. Cell Biol.* 98:1591–1596. doi:10.1083/jcb.98.4.1591

Kim, J., J.E. Lee, S. Heynen-Genel, E. Suyama, K. Ono, K. Lee, T. Ideker, P. Aza-Blanc, and J.G. Gleeson. 2010. Functional genomic screen for modulators of ciliogenesis and cilium length. *Nature*. 464:1048–1051. doi:10.1038/nature08895

Kim, J.C., J.L. Badano, S. Sibold, M.A. Esmail, J. Hill, B.E. Hoskins, C.C. Leitch, K. Venner, S.J. Ansley, A.J. Ross, et al. 2004. The Bardet-Biedl protein BBS4 targets cargo to the pericentriolar region and is required for microtubule anchoring and cell cycle progression. *Nat. Genet.* 36:462–470. doi:10.1038/ng1352

Kovacs, J.J., E.J. Whalen, R. Liu, K. Xiao, J. Kim, M. Chen, J. Wang, W. Chen, and R.J. Lefkowitz. 2008. Beta-arrestin-mediated localization of smoothened to the primary cilium. *Science*. 320:1777–1781. doi:10.1126/science.1157983

Lauffer, B.E.L., S. Chen, C. Melero, T. Kortemme, M. von Zastrow, and G.A. Vargas. 2009. Engineered protein connectivity to actin mimics PDZ-dependent recycling of G protein-coupled receptors but not its regulation by Hrs. *J. Biol. Chem.* 284:2448–2458. doi:10.1074/jbc.M806370200

Li, Y., J. Li, S.W. Straight, and D.B. Kershaw. 2002. PDZ domain-mediated interaction of rabbit podocalyxin and Na(+)/H(+) exchange regulatory factor-2. *Am. J. Physiol. Renal Physiol.* 282:F1129–F1139.

Maday, S., E. Anderson, H.C. Chang, J. Shorter, A. Satoh, J. Sfakianos, H. Fölsch, J.M. Anderson, Z. Walther, and I. Mellman. 2008. A PDZ-binding motif controls basolateral targeting of syndecan-1 along the biosynthetic pathway in polarized epithelial cells. *Traffic*. 9:1915–1924. doi:10.1111/j.1600-0854.2008.00805.x

Meder, D., A. Shevchenko, K. Simons, and J. Füllekrug. 2005. Gp135/podocalyxin and NHERF-2 participate in the formation of a preapical domain during polarization of MDCK cells. *J. Cell Biol.* 168:303–313. doi:10.1083/jcb.200407072

Mellman, I., and W.J. Nelson. 2008. Coordinated protein sorting, targeting and distribution in polarized cells. *Nat. Rev. Mol. Cell Biol.* 9:833–845. doi:10.1038/nrm2525

Milenkovic, L., M.P. Scott, and R. Rohatgi. 2009. Lateral transport of Smoothened from the plasma membrane to the membrane of the cilium. *J. Cell Biol.* 187:365–374. doi:10.1083/jcb.200907126

Nachury, M.V., A.V. Loktev, Q. Zhang, C.J. Westlake, J. Peränen, A. Merdes, D.C. Slusarski, R.H. Scheller, J.F. Bazan, V.C. Sheffield, and P.K. Jackson. 2007. A core complex of BBS proteins cooperates with the GTPase Rab8 to promote ciliary membrane biogenesis. *Cell*. 129:1201–1213. doi:10.1016/j.cell.2007.03.053

Nielsen, J.S., M.L. Graves, S. Chelliah, A.W. Vogl, C.D. Roskelley, and K.M. McNagny. 2007. The CD34-related molecule podocalyxin is a potent inducer of microvillus formation. *PLoS ONE*. 2:e237. doi:10.1371/journal.pone.0000237

Patel, A., and E. Honoré. 2010. Polycystins and renovascular mechanosensory transduction. *Nat. Rev. Nephrol.* 6:530–538. doi:10.1038/nrneph.2010.97

Reczek, D., and A. Bretscher. 1998. The carboxyl-terminal region of EBP50 binds to a site in the amino-terminal domain of ezrin that is masked in the dormant molecule. *J. Biol. Chem.* 273:18452–18458. doi:10.1074/jbc.273.29.18452

Reczek, D., M. Berryman, and A. Bretscher. 1997. Identification of EBP50: A PDZ-containing phosphoprotein that associates with members of the ezrin-radixin-moesin family. *J. Cell Biol.* 139:169–179. doi:10.1083/jcb.139.1.169

Rogers, K.K., P.D. Wilson, R.W. Snyder, X. Zhang, W. Guo, C.R. Burrow, and J.H. Lipschutz. 2004. The exocyst localizes to the primary cilium in MDCK cells. *Biochem. Biophys. Res. Commun.* 319:138–143. doi:10.1016/j.bbrc.2004.04.165

Rohatgi, R., L. Milenkovic, R.B. Corcoran, and M.P. Scott. 2009. Hedgehog signal transduction by Smoothened: pharmacologic evidence for a 2-step activation process. *Proc. Natl. Acad. Sci. USA*. 106:3196–3201. doi:10.1073/pnas.0813373106

Schmieder, S., M. Nagai, R.A. Orlando, T. Takeda, and M.G. Farquhar. 2004. Podocalyxin activates RhoA and induces actin reorganization through NHERF1 and Ezrin in MDCK cells. *J. Am. Soc. Nephrol.* 15:2289–2298. doi:10.1097/01.ASN.0000135968.49899.E8

Sfakianos, J., A. Togawa, S. Maday, M. Hull, M. Pypaert, L. Cantley, D. Toomre, and I. Mellman. 2007. Par3 functions in the biogenesis of the primary cilium in polarized epithelial cells. *J. Cell Biol.* 179:1133–1140. doi:10.1083/jcb.200709111

Sorokin, S. 1962. Centrioles and the formation of rudimentary cilia by fibroblasts and smooth muscle cells. *J. Cell Biol.* 15:363–377. doi:10.1083/jcb.15.2.363

Takeda, T., T. McQuistan, R.A. Orlando, and M.G. Farquhar. 2001. Loss of glomerular foot processes is associated with uncoupling of podocalyxin from the actin cytoskeleton. *J. Clin. Invest.* 108:289–301.

Terawaki, S., R. Maesaki, K. Okada, and T. Hakoshima. 2003. Crystallographic characterization of the radixin FERM domain bound to the C-terminal region of the human Na+/H+-exchanger regulatory factor (NHERF). *Acta Crystallogr. D Biol. Crystallogr.* 59:177–179. doi:10.1107/S0907444902019686

Vieira, O.V., K. Gaus, P. Verkade, J. Fullekrug, W.L.C. Vaz, and K. Simons. 2006. FAPP2, cilium formation, and compartmentalization of the apical membrane in polarized Madin-Darby canine kidney (MDCK) cells. *Proc. Natl. Acad. Sci. USA*. 103:18556–18561. doi:10.1073/pnas.0608291103

Wang, Y., Z. Zhou, C.T. Walsh, and A.P. McMahon. 2009. Selective translocation of intracellular Smoothened to the primary cilium in response to Hedgehog pathway modulation. *Proc. Natl. Acad. Sci. USA*. 106:2623–2628. doi:10.1073/pnas.0812110106

Winckler, B., P. Forscher, and I. Mellman. 1999. A diffusion barrier maintains distribution of membrane proteins in polarized neurons. *Nature*. 397:698–701. doi:10.1038/17806

Yoshimura, S., J. Egerer, E. Fuchs, A.K. Haas, and F.A. Barr. 2007. Functional dissection of Rab GTPases involved in primary cilium formation. *J. Cell Biol.* 178:363–369. doi:10.1083/jcb.200703047

Yu, C.Y., J.Y. Chen, Y.Y. Lin, K.F. Shen, W.L. Lin, C.L. Chien, M.B.A. ter Beest, and T.S. Jou. 2007. A bipartite signal regulates the faithful delivery of apical domain marker podocalyxin/Gp135. *Mol. Biol. Cell*. 18:1710–1722. doi:10.1091/mbc.E06-07-0629

Yun, C.H., G. Lamprecht, D.V. Forster, and A. Sidor. 1998. NHE3 kinase A regulatory protein E3KARP binds the epithelial brush border Na+/H+ exchanger NHE3 and the cytoskeletal protein ezrin. *J. Biol. Chem.* 273:25856–25863. doi:10.1074/jbc.273.40.25856

Zhu, A.J., L. Zheng, K. Suyama, and M.P. Scott. 2003. Altered localization of *Drosophila* Smoothened protein activates Hedgehog signal transduction. *Genes Dev.* 17:1240–1252. doi:10.1101/gad.1080803

Zuo, X., W. Guo, and J.H. Lipschutz. 2009. The exocyst protein Sec10 is necessary for primary ciliogenesis and cystogenesis in vitro. *Mol. Biol. Cell*. 20:2522–2529. doi:10.1091/mbc.E08-07-0772